Published in IET Radar, Sonar and Navigation
Received on 14th June 2013
Revised on 19th September 2013
Accepted on 23rd October 2013
doi: 10.1049/iet-rsn.2013.0207

Special Issue: Bistatic and MIMO radars and their applications in surveillance and remote sensing

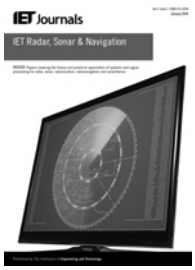

ISSN 1751-8784

Two-dimensional location of moving targets within local areas using WiFi-based multistatic passive radar

Paolo Falcone, Fabiola Colone, Antonio Macera, Pierfrancesco Lombardo

DIET Department, University of Rome 'La Sapienza', Via Eudossiana, 18–00184 Rome, Italy
E-mail: lombardo@infocom.uniroma1.it

Abstract: In this study the authors investigate the two-dimensional target localisation capabilities of a passive radar system based on WiFi transmissions. It is well known that the most straightforward way to achieve the target position estimation in the horizontal plane with a passive radar exploits the measurements either of a single bistatic range plus a direction of arrival (DoA) or of two bistatic ranges collected by two separate receivers. However, for a practical application it is interesting to clearly define which one of the two approaches provides the passive radar target localisation with a higher accuracy and whether combining both multiple bistatic range plus DoA measurements provides a further advantage. A multistatic configuration is considered which allows to collect a set of range/Doppler/angle measurements for a given target. Different target localisation strategies are devised and compared, based on subsets of the available measurements with the aim of understanding the localisation accuracies achievable using the different combinations of measurements. Experimental results are shown based on a passive radar prototype developed and fielded at the DIET Department – Sapienza University of Rome. This will contribute to demonstrate the fruitful application of the passive radar concept for short range surveillance.

1 Introduction

In the last years the interest in passive coherent location (PCL) radar for surveillance purposes has significantly grown up [1, 2]. In particular, a number of studies have looked at the use of PCL radar systems for local area monitoring applications by exploiting wireless network transmissions as potential sources of opportunity.

Among them, transmitters for base stations of global system for mobile Communications, Universal Mobile Telecommunications System, Worldwide Interoperability for Microwave Access (WiMAX) and forthcoming generation, such as Long Term Evolution, of mobile personal communication and network connection provide a largely populated and well-connected network of sources of opportunity for medium range surveillance [3–11].

In contrast, the IEEE 802.11 Standard based (WiFi) transmitters provide a very local but potentially wide bandwidth and well-controlled signals useful when aiming at indoor surveillance or at monitoring small external areas [12]. These signals have been shown to be an appropriate choice for the detection and localisation of designated vehicles, human beings or man-made objects within short ranges using the passive radar principle [13, 14]. For example, the WiFi-based passive radar can be employed for detecting and tracking people moving inside a building after a disaster, for monitoring vehicles moving in parking areas, or for the surveillance of sensible areas within railway station, airport terminals and private commercial premises [15].

Effective processing techniques have been designed to enable the practical operation of the resulting system [13, 15–22], and to rise the specific challenges issued by advanced applications, such as target cross-range profiling via ISAR processing [23–26].

With reference to the target localisation stage, the preliminary results reported in [21, 22] show that it is possible to estimate the target x-y coordinates with reasonable accuracy. To this purpose, multiple passive radar sensors can be exploited which allow to collect a set of range/Doppler measures for the same target which is observed at different bi-static geometries. Moreover, assuming that each sensor uses a couple of surveillance antennas, a simple interferometric approach can be exploited to estimate the direction of arrival (DoA) of the target echo. This obviously increases the set of available measures thus potentially improving the localisation capability of the conceived system.

However, different measures (range/Doppler/DoA) might be characterised by different accuracies and their effect on the target two-dimensional (2D) localisation might be highly dependent on the target geometry. Moreover the availability of multiple measures is typically paid in terms of system complexity and cost.

Therefore in this paper we consider the problem of obtaining the target x-y coordinates from a small set of measures. In particular, we carefully analyse the benefits deriving from the inclusion of a given measure in the set exploited for target localisation since this allows to give hints to the design of

the conceived multistatic system. Moreover, proper localisation strategies are presented to obtain the best localisation performance from the joint exploitation of all the available measures. Finally, different approaches are investigated for the estimation of the target motion components; this might fruitfully feed the target tracking algorithm or it can effectively initialise the target motion parameters estimation stage needed for its ISAR profile formation [23].

The experimental results are shown against the data collected by the WiFi-based passive radar prototype developed at the DIET Dept. – University of Rome 'La Sapienza'. Specifically the results are reported for different tests performed using vehicular targets in a wide outdoor area. The availability of the ground truth provided by a global positioning system (GPS) receiver with real time Kinematic allows us to compare the considered localisation strategies by evaluating the achievable accuracies and therefore to assess which ones are the configurations to be preferred when designing a practical short range passive radar scheme aiming at localising the targets.

The paper is organised as follows. In Section 2 the WiFi-based passive radar scheme is briefly described together with the main processing stages required to collect the range/Doppler/DoA measures. Also the prototype used for the experimental activity is introduced. In Section 3 the exploitation of a minimum number of measures is considered for target 2D localisation and the results are compared when using two range measures from two PCL systems or the range/DoA couple provided by a single PCL system. The possibility of jointly exploiting all the available measures is investigated in Section 4 where a Maximum Likelihood estimation approach is presented which is shown to significantly improve the target localisation performance. The target motion parameters estimation is addressed in Section 5. Finally, in Section 6 we draw our conclusions.

2 WiFi-based passive radar concept and the experimental setup

A WiFi access point (AP), used to provide coverage for an assigned area, potentially acts as an ideal illuminator of opportunity for short range PCL surveillance if appropriate techniques are adopted to process the collected signals. This has been largely demonstrated in [12–22] by means of both theoretical and experimental results.

Specifically the processing scheme for target detection designed by the authors has been fully described in [13] and its main blocks are depicted in Fig. 1.

The low-power signal reflected from the target is collected by the main PCL receiver (typically known as the surveillance channel) using a directive antenna steered towards the surveillance area. An auxiliary receiver (typically known as the reference channel) is usually adopted to collect the transmitted signal.

A transmitter-specific conditioning of the reference signal is first performed to improve the resulting ambiguity function (AF); to this purpose proper techniques have been introduced to cope with the high sidelobe structures appearing in the AF of WiFi signals based on different modulations [13, 15–18].

The pre-conditioned reference signal is then used to remove undesired contributions (direct signal leakage and strong clutter/multipath echoes) that have been received, along with the moving target echo, on the surveillance channel. To this purpose we resort to a modified version of the adaptive cancellation approach presented in [27], the extensive cancellation algorithm (ECA), which operates by subtracting from the surveillance signal properly scaled and delayed replicas of the reference signal. Specifically, the Batches version of the ECA (ECA-B) is adopted which requires the filter weights to be estimated over smaller portions of the integration time.

After the cancellation stage, the detection process is based on the evaluation of the bistatic two-dimensional (range-Doppler) cross-correlation function (2D-CCF) between the surveillance and the reference signal. Based on the pulsed nature of WiFi transmissions and observing that the pulse duration is significantly smaller than the coherent processing interval required to achieve the desired signal-to-noise ratio (SNR) and Doppler resolution for the considered applications, the 2D-CCF can be practically evaluated by cross-correlating the surveillance signal with the reference signal on a pulse basis ('Range compression' block in Fig. 1) and coherently integrating the obtained results over consecutive pulses ('2D-CCF evaluation' block in Fig. 1). At this latter stage, an ad hoc designed taper function can be exploited to control the sidelobes of the AF in the Doppler dimension [19].

A constant false alarm rate (CFAR) threshold can be then applied on the obtained map to automatically detect the potential targets according to a specific CFAR detection scheme. This provides a first target localisation over the bistatic range/Doppler plane.

The measures collected at consecutive observations can be used to perform a line tracking over this plane. Using a conventional Kalman algorithm allows to reduce the false alarm rate whereas yielding more accurate range/velocity estimations.

Assuming that the PCL system is equipped with a couple of surveillance antennas, the same processing scheme might be applied on both channels and an interferometric approach can be exploited to estimate the DoA of the detected target echo.

Combining the available measures or, possibly, using the measures obtained from multiple PCL systems, the target 2D localisation in local Cartesian coordinates can be obtained.

The results obtained with the above processing scheme have been reported in many contributions showing its

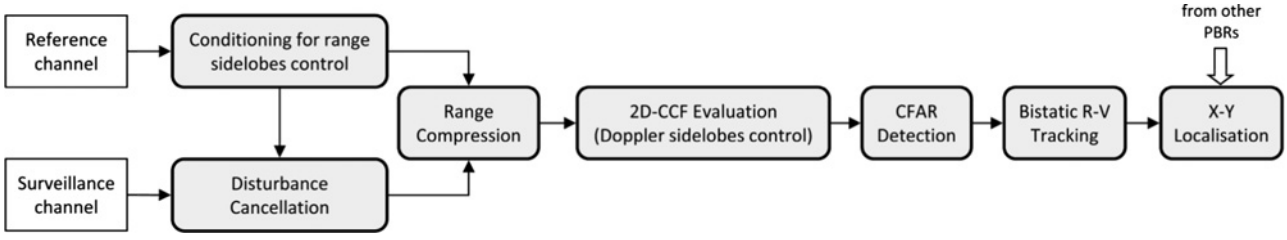

Fig. 1 *WiFi-based PCL processing scheme for target detection and localisation*

doi: 10.1049/iet-rsn.2013.0207

effectiveness against typical scenarios [13, 15–17, 21, 22]. Some examples are reported in the following using the real data set that will be then exploited in the subsequent Sections to investigate different localisation strategies and to assess their performance.

The considered data set has been collected by means of the experimental setup sketched in Fig. 2; the reported test was performed in a parking area where a vehicular target was employed moving on a given trajectory (see the left-hand side of Fig. 2). A GPS receiver was mounted on the moving car to collect the ground truth.

A commercial WiFi AP was used as transmitter of opportunity. Its antenna output was connected to the transmitting antenna (TX) that was located at the point represented with the coordinates $(x_{TX}, y_{TX}) = (0, 0)$ m; a directional coupler was used to send a −20 dB copy of the transmitted signal to the first receiving channel of a four-channel receiving system with the aim of collecting the reference signal. Note that this approach allows to recover a quite pure copy of the transmitted signal by exploiting a partially cooperative AP. Alternatively the reference signal might be collected by a dedicated antenna or recovered from the signal received at the surveillance channel, [13]; in these cases proper techniques can be applied to remove undesired effects because of multipath contributions, [13].

Three surveillance antennas were directly connected to the three remaining receiving channels. Note that, using the three available surveillance channels, we could synthesise two independent PCL sensors one of which is equipped with a pair of surveillance antennas providing the target DoA estimation capability. To this purpose, the first standalone surveillance antenna (RX 1) was located in $(x_1, y_1) = (25, 0)$ m in a bistatic configuration with respect to the TX; on the other hand antennas RX 2 and RX 3 were placed a few tens of centimeters below the TX (in a quasi-monostatic configuration), displaced in the horizontal direction by 12 cm which gives a 45° ambiguity for the DoA estimation.

After a fully coherent base-band down-conversion stage, the signals collected at the different receiving channels are sampled at 22 MHz and stored for off-line processing.

The WiFi-based passive radar processing scheme depicted in Fig. 1 is applied against the collected surveillance signals separately at each receiving channel. In particular, the ECA is applied with a batch duration equal to 100 ms over a range of 300 m; a coherent integration time of 0.5 s is used to evaluate the 2D-CCF over consecutive portions of the acquired signals (frames) with a fixed displacement of 0.1 s (10 frames per second are thus obtained); and target detection is performed by resorting to a standard cell-average CFAR threshold with a probability of false alarm equal to 10^{-4}.

Fig. 3 reports the detection results obtained for the two PCL systems for a 15 s acquisition (150 Frames) compared with the ground truth (black discontinuous line). Specifically, the output is shown of a standard association stage only aimed at discarding false alarms; moreover the detections associated to stationary tracks have been discarded since they are likely to correspond to clutter residues. The raw target plots are reported since the obtained measures have not been filtered at this stage.

In particular Fig. 3*a* reports the results for the PCL system based on the standalone antenna RX1, namely PCL1. The results for PCL2 are shown in Fig. 3*b* where a two-out-of-two criterion has been adopted on the detection results separately obtained against the signals collected by antennas RX2 and RX3.

As is apparent, many plots are obtained that clearly correspond to the target echoes. In addition a long plot sequence is detected by both PCL1 and PCL2 that is likely to be generated by the double-bounce reflection of the target echo over the building in the upper zone of Fig. 2 (see the sequence of detections at positive Doppler frequency and decreasing bistatic range between 250 and 150 m). In practical applications, the false targets generated by multipath effect on the target echo might be reasonably recognised if the true target is correctly detected and tracked and the a-priori knowledge of the stationary scene is available, namely the shape and position of the main stationary obstacles forming the observed scene. In fact, based on geometrical considerations and assuming a simple propagation model, it is possible in principle to identify and discard the target tracks that are likely to correspond to multiple-bounce echoes.

For the purpose of our analysis the nearest sequence of plots is selected which clearly corresponds to the employed target. This procedure has been partially automatised by applying a conventional tracking stage on the range/Doppler plane (see Section 3.2) and then manually extracting the track of interest; specifically the (possibly filtered) plots associated to the selected track are collected which represent a set of bistatic range and Doppler frequency measurements (namely, R_{B1} and f_{D1}), for the considered

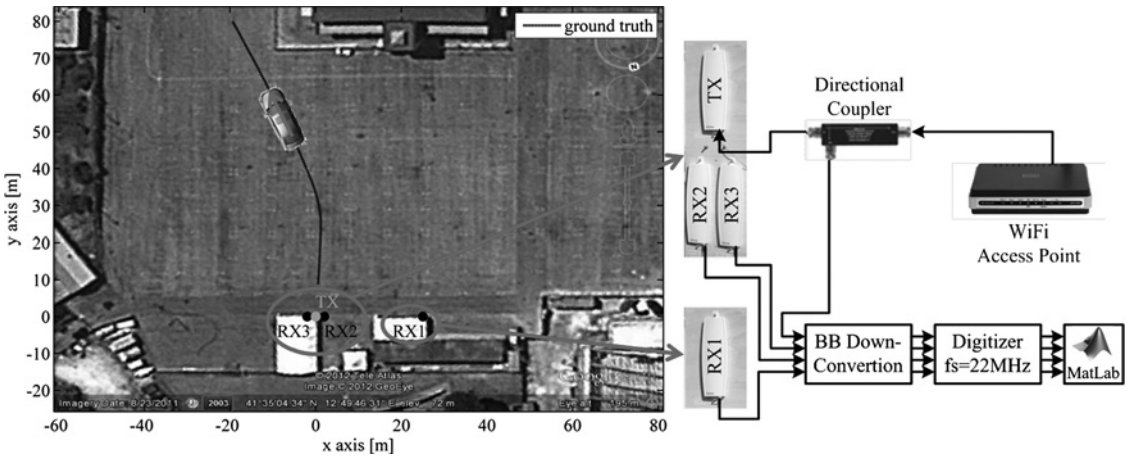

Fig. 2 *Sketch of the experimental setup and the performed test*

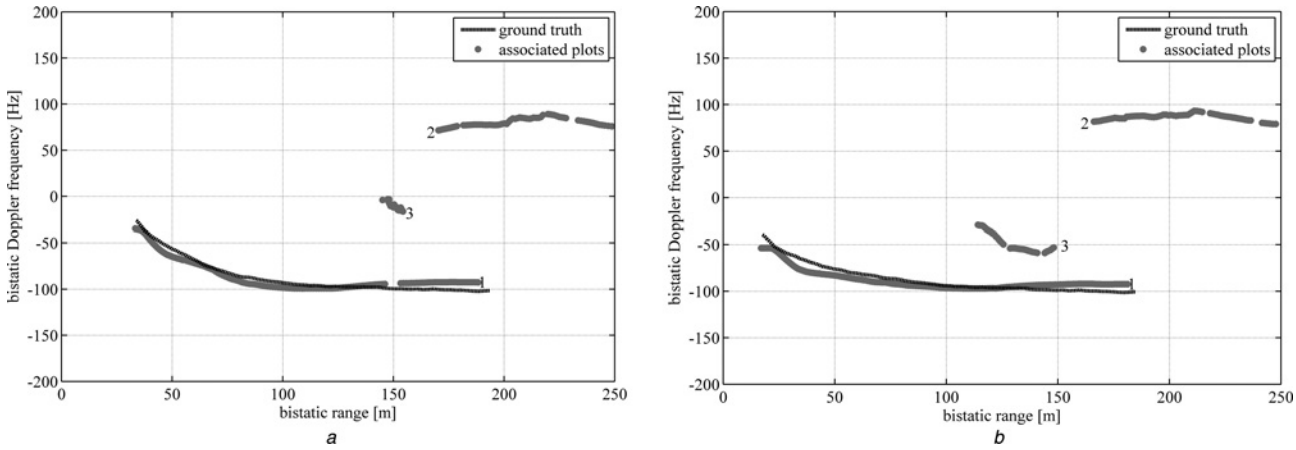

Fig. 3 *Detection results after association stage over the bistatic range/Doppler plane for*
a PCL1
b PCL2

target, performed by PCL1 along the acquisition. Similarly, the set of range/Doppler measures is collected for PCL2 (R_{B2} and f_{D2}); in this case, also the phase difference between RX 2 and RX 3 measured at the target detection point is exploited to obtain the target DoA estimation. The estimated target DoA along the performed acquisition is show in Fig. 4, compared with the ground truth showing that it is well in line with the test geometry.

Although the reported analysis is limited to the employed target track, in practical applications all the tracks identified by the exploited systems would be given as input to the 2D localisation stage. In this regard, also the association of tracks from different PCL need to be automatised; in [28, 29] possible approaches to passive multi-static multi-target tracking are presented and the challenging task of tracks association is properly dealt with.

In the following Section the collected target measurements will be exploited to obtain effective target localisation over the *x*-*y* plane.

3 Target localisation using a minimum number of measures

Once a target has been detected in the bistatic range/Doppler plane, its 2D localisation might be desirable in an assigned area, where a *x*-*y* orthogonal coordinate system is defined. A minimum number of two position dependent measurements is required to perform the 2D target localisation. However different sets of two measurements could be exploited and this choice has implications both on the resulting localisation accuracy and on the PCL system to be designed there including the number and displacement of the receivers and the number of receiving antennas for each passive receiver.

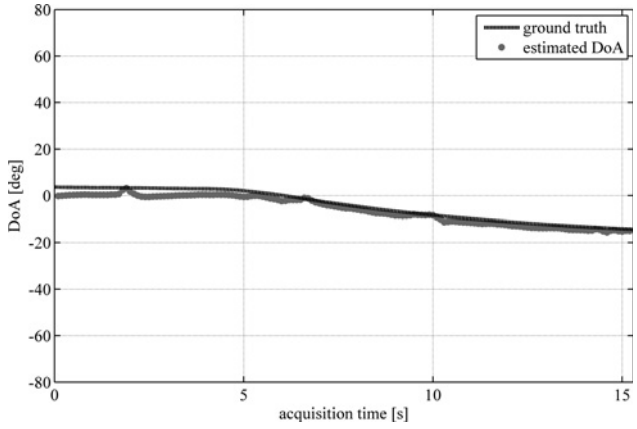

Fig. 4 *Target DoA measures obtained by PCL2*

With reference to our experimental setup, the target 2D localisation can be performed by using:

(A) two bistatic range measurements provided by two PCL receivers after the detection stage
(B) two bistatic range measurements obtained from two PCL receivers after a range/Doppler tracking stage
(C) a range measurement and a DoA measurement provided by a single PCL system.

In the following of this section these approaches are investigated and compared, whereas in a subsequent section we consider the possibility to exploit all available information.

3.1 Using raw range measurements from two PCL systems

As is well known, for a given PCL system with known transmitter and receiver locations, a bistatic range measure univocally identifies the ellipse where the target lies. The intersection points of two ellipses provide the estimation of up to four possible target positions over the *x*-*y* plane. The ambiguous solutions might be discarded by forcing the target to be within the antennas' main lobe; this presumes some degree of a priori knowledge, namely information about the area covered by transmitting and receiving antennas beams should be available.

The achievable target localisation accuracy depends on both the range measures accuracy and on the additional multiplicative effect caused by the multistatic system geometry on the achievable precision; the latter effect is known as the dilution of precision (DOP) factor in GPS and geomatics engineering [30].

As an example, the result obtained for the considered experiment is reported in Fig. 5; the white dots represent the estimated target positions at consecutive acquisition frames when using the raw range measures extracted from

doi: 10.1049/iet-rsn.2013.0207

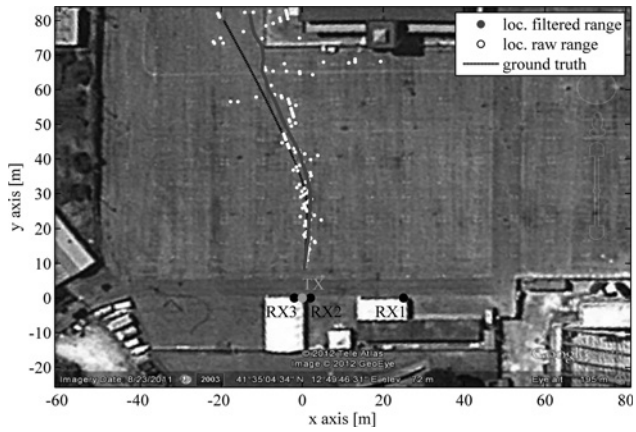

Fig. 5 *Target localisation using two bistatic range measures*

Figs. 3*a* and *b* for PCL1 and PCL2. As is apparent, localisation errors in the order of metres are experienced along the x dimension whereas the track follows the actual motion of the target along the y dimension (which is oriented along the range axis). In particular, the worst localisation performance is experienced when the target is far from the surveillance antennas. In fact, in such locations the bistatic ellipses become quite similar and almost tangent, thus increasing the DOP factor along the x dimension.

Table 1 summarises the localisation performance in terms of positioning error defined as $\varepsilon_P = \sqrt{\varepsilon_x^2 + \varepsilon_y^2}$ where ε_x and ε_y are the errors along the x and y dimensions, respectively. In particular, the results obtained with the above approach exploiting two raw range measurements are reported in the first row of Table 1.

3.2 Using filtered range measurements from two PCL systems

In [21] we have shown that target localisation performance of the conceived WiFi based PCL system might be significantly improved if the target range measurements are used at the output of a dynamics model-based filtering stage that takes into account the multiple sequential measurements. To this aim, in the following a conventional Kalman tracking algorithm is applied over the range/Doppler plane separately for each PCL receiver.

In particular, the algorithm operates in conjunction with a nearest neighbour association strategy. A parabolic motion model is assumed for the target over the bistatic range/Doppler plane which results in a 3×1 system state vector (range, Doppler, Doppler rate); this model is representative for a target moving in the surveillance space with uniform linear motion. The noise affecting the collected measures (bistatic range and Doppler) is assumed to be Gaussian distributed with zero mean and variances σ_R^2 and σ_D^2. The measurements accuracies are evaluated in practice as $\sigma_R^2 = \Delta_R^2/\text{SNR}$ and $\sigma_D^2 = \Delta_D^2/\text{SNR}$, respectively, where Δ_R and Δ_D are the achievable range and Doppler resolutions and the SNR can be estimated at the target detection point over the range/Doppler map.

Note that a range/Doppler tracking stage is usually adopted in passive radar applications because it allows both to discard false alarms and to improve the range measure accuracy prior to merging the results from multiple PCL receivers, [1, 2]. In fact, after the line tracking, also the target bistatic Doppler measurements are indirectly exploited to obtain more accurate range measurements with respect to the raw case. As a consequence, the localisation procedure based on the intersection of the corresponding ellipses yields a much more stable estimation of the target position in the x-y plane.

The result is reported for comparison in Fig. 5 (dark dots). As is apparent, the resulting track is almost identical to the actual path of the car; the slight differences are because of clutter residuals which affect the estimation of the target range and Doppler frequency, especially when it approaches the building in the parking area. Correspondingly the localisation accuracy is significantly improved since the standard deviation of the positioning error is reduced by 4.2 m with respect to the previous case (see second row of Table 1). Obviously, better results could be obtained by applying a second tracking stage over the x-y plane; however we are interested in the direct impact of the available measures on the 2D localisation capability of the system so that the comparison is performed without a target tracking in the x-y plane.

3.3 Using range and DoA measurements from a single PCL system

An alternative approach to target 2D localisation consists in the exploitation of the bistatic range and DoA measures provided by a single PCL receiver equipped with a couple of surveillance antennas. With reference to our experimental setup we could use the filtered bistatic range measures and the DoA estimates provided by PCL2.

The target position is obtained by intersecting the bistatic ellipse with the line identifying the DoA of the target echo. Note that ambiguous solutions might be found using this approach, as well as when exploiting two range measurements, because the DoA measurement could be ambiguous itself. With particular reference to our case study, the horizontal displacement of the receiving antennas (12 cm) yields a 45° ambiguity for the DoA estimation.

Table 1 Target localisation performance using different strategies

Reference paper section	Exploited measurements and method	Maximum positioning error, m	Mean positioning error, m	Positioning error standard deviation, m
Section 3.1	2 raw range measurements	32.65	4.81	5.78
Section 3.2	2 filtered range measurements	6.64	2.47	1.53
Section 3.3	1 filtered range & 1 DoA measurements	2.56	1.79	0.54
Section 4.1	2 filtered ranges & 1 DoA measurements – LS approach	7.04	2.10	1.77
Section 4.2	2 filtered ranges & 1 DoA measurements – ML approach	2.37	1.6	0.49

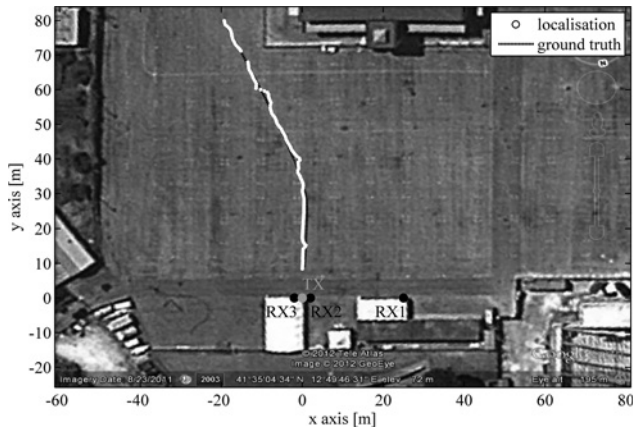

Fig. 6 *Target localisation using bistatic range + DoA from PCL2*

Nevertheless, since directive antennas are employed, the ambiguous solutions can be discarded by forcing the target to be within the area covered by the antennas' main lobe.

Again the achievable localisation accuracy depends both on the accuracy of the exploited measures and on the PCL/target geometry. For example, the performance is expected to rapidly get worse as the target moves away from the receiver; basically this is because of the decrease in the target echo power level and to the widening of the uncertainty x-y area caused by a given DoA error.

The target localisation results for this approach are shown in Fig. 6 whereas the third row of Table 1 summarises the obtained performance. As is apparent, the exploitation of the quite accurate phase difference measurement allows to further improve the target localisation accuracy. Basically the maximum positioning error along the target trajectory is now comparable with the target size.

Based on the previous analysis, we might gather that, despite the simple approach exploited for DoA estimation (i.e. phase difference measurement between a couple of surveillance antennas), the target localisation based on (at least) one angular measurement yields more reliable performance. This is a quite interesting result because it contrasts with the typical case of other PCL systems operating at lower carrier frequencies for which the DoA estimation tends to be unstable and inaccurate. Moreover, this directs the design of a multistatic WiFi-based PCL system to the inclusion of few sensors equipped with multiple receiving antennas instead of many lower-cost sensors using a single surveillance antenna.

4 Target localisation using multiple measurements

The availability of multiple measurements about the target obtained from different PCL receivers might potentially yield improved localisation performance if properly exploited.

With reference to our experimental setup, the target 2D localisation can be performed by jointly using the target DoA measurement provided by PCL2 and the two bistatic range measurements provided by PCL1 and PCL2. In the following two different approaches are investigated and compared.

4.1 Least square solution

Aiming at the 2D localisation of the target, the exploitation of range and DoA measurements from multiple PCL receivers requires the solution of a system of N non-linear equations in two unknowns.

In our case $N = 3$ and, based on the quasi-monostatic configuration of PCL2, we obtain

$$\begin{cases} R_{B1} = f_{R1}(x_t, y_t) = \sqrt{(x_{\mathrm{TX}} - x_t)^2 + (y_{\mathrm{TX}} - y_t)^2} \\ \quad + \sqrt{(x_1 - x_t)^2 + (y_1 - y_t)^2} \\ R_{B2} = f_{R2}(x_t, y_t) = 2\sqrt{(x_{\mathrm{TX}} - x_t)^2 + (y_{\mathrm{TX}} - y_t)^2} \\ \vartheta = f_{\vartheta}(x_t, y_t) = \arctan(x_t / y_t) \end{cases} \tag{1}$$

where:

- $\boldsymbol{p} = [x_t, y_t]^{\mathrm{T}}$ are the target coordinates
- R_{B1} and R_{B2} are the bistatic ranges given by PCL1 and PCL2, respectively; and
- ϑ is the target angle of arrival given by PCL2.

The system in (1) can be linearised by using a first-order Taylor series approximation about the target tentative position $\boldsymbol{p}_0 = [x_{t0}, y_{t0}]^{\mathrm{T}}$

$$\boldsymbol{m} \cong \boldsymbol{m}_0 + \boldsymbol{H} \cdot (\boldsymbol{p} - \boldsymbol{p}_0) \tag{2}$$

where a matrix notation has been adopted based on the following definitions

$$\boldsymbol{m} = \begin{bmatrix} R_{B1} & R_{B2} & \vartheta \end{bmatrix}^{\mathrm{T}} \tag{3}$$

$$\begin{aligned} \boldsymbol{m}_0 &= \begin{bmatrix} R_{B1,0} & R_{B2,0} & \vartheta_0 \end{bmatrix}^{\mathrm{T}} \\ &= \begin{bmatrix} f_{R1}(x_{t0}, y_{t0}) & f_{R2}(x_{t0}, y_{t0}) & f_{\vartheta}(x_{t0}, y_{t0}) \end{bmatrix}^{\mathrm{T}} \end{aligned} \tag{4}$$

$$\boldsymbol{H} = \begin{bmatrix} \left.\frac{\partial f_{R1}}{\partial x}\right|_{(x_{t0}, y_{t0})} & \left.\frac{\partial f_{R1}}{\partial x}\right|_{(x_{t0}, y_{t0})} \\ \left.\frac{\partial f_{R2}}{\partial x}\right|_{(x_{t0}, y_{t0})} & \left.\frac{\partial f_{R2}}{\partial y}\right|_{(x_{t0}, y_{t0})} \\ \left.\frac{\partial f_{\vartheta}}{\partial x}\right|_{(x_{t0}, y_{t0})} & \left.\frac{\partial f_{\vartheta}}{\partial y}\right|_{(x_{t0}, y_{t0})} \end{bmatrix} \tag{5}$$

Therefore the least square (LS) solution of the system in (2) is given by

$$\boldsymbol{p} = (\boldsymbol{H}^{\mathrm{T}}\boldsymbol{H})^{-1}\boldsymbol{H}^{\mathrm{T}}(\boldsymbol{m} - \boldsymbol{m}_0) + \boldsymbol{p}_0 \tag{6}$$

where the pseudo-inverse of matrix $\boldsymbol{H}$ has been exploited. This allows to update the target coordinates with respect to the tentative position and to reiterate the procedure until the displacement $\|\boldsymbol{p} - \boldsymbol{p}_0\|$ is within the requirements on the positioning accuracy or the maximum admitted number of iterations is reached.

In the hypothesis of error free measurements, this algorithm converges to the true target position. Obviously, the passive radar measurements suffer from unknown errors $\boldsymbol{\varepsilon}_{\mathrm{M}} = \hat{\boldsymbol{m}} - \boldsymbol{m}$; under the hypothesis of small errors, the linearisation procedure described above can be exploited (around the true target position) to evaluate how these errors reflect on the estimated target position. Specifically it is easy to verify that the covariance matrix $\boldsymbol{\Sigma}_{\mathbf{P}}$ of the

doi: 10.1049/iet-rsn.2013.0207

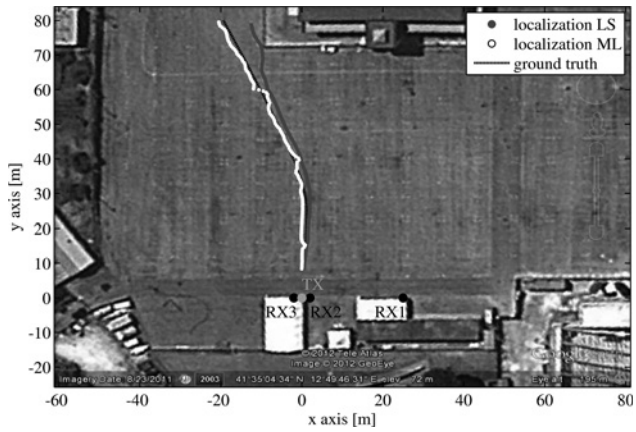

Fig. 7 *Target localisation using two range measurements + DoA*

corresponding positioning error over the *x-y* plane is given by

$$\boldsymbol{\Sigma}_{\mathrm{P}} = E\{\boldsymbol{\varepsilon}_P \boldsymbol{\varepsilon}_P^{\mathrm{T}}\} = (\boldsymbol{H}^{\mathrm{T}}\boldsymbol{H})^{-1}\boldsymbol{H}^{\mathrm{T}}\boldsymbol{\Sigma}_{\mathrm{M}}\boldsymbol{H}(\boldsymbol{H}^{\mathrm{T}}\boldsymbol{H})^{-1} \quad (7)$$

where $\boldsymbol{\Sigma}_{\mathrm{M}}$ is the covariance matrix of the errors affecting the performed measurements.

The results obtained against the available data set are reported in Fig. 7 (using dark dots) and the corresponding performance are summarised in Table 1 for comparison.

As is apparent, the direct exploitation of all the available measurements causes a degradation of the localisation performance with respect to the use of the minimum required number of measurements. Specifically the standard deviation of the positioning accuracy is three times greater than using a single range measurement and the DoA measurement. In facts, the inclusion of an additional range measurement with low accuracy yields worse performance because the system equally relies on the available measurements.

This is not surprising since the LS estimation procedure coincides with a maximum likelihood (ML) estimator of the target position whenever the joint probability density function of the available measurements is Gaussian distributed with identical variances. However, this does not apply to our localisation problem being each measurement characterised by its own accuracy. In facts, we are exploiting non-homogeneous measurements (i.e. range and DoA) and these are provided by PCL sensors operating with different geometries, thus experiencing different SNR values and DOP factors.

The above considerations should be taken into account in order to better exploit the collected measurements, thus making it possible to improve the achievable localisation performance. To accomplish such result, a true ML estimator should be employed along the line described in the next Section.

4.2 Maximum likelihood estimator

Under the hypothesis of small errors $\boldsymbol{\varepsilon}_{\mathrm{M}}$ affecting the performed measurements $\hat{\boldsymbol{m}}$, the linearisation in (2) can be exploited

$$\hat{\boldsymbol{m}} = \boldsymbol{m} + \boldsymbol{\varepsilon}_{\mathrm{M}} = \boldsymbol{m}_0 + \boldsymbol{H}\cdot(\boldsymbol{p}-\boldsymbol{p}_0) + \boldsymbol{\varepsilon}_{\mathrm{M}} \quad (8)$$

Moreover let us assume that the joint probability density function of the errors $\boldsymbol{\varepsilon}_{\mathrm{M}}$ is Gaussian with zero mean value and covariance matrix $\boldsymbol{\Sigma}_{\mathrm{M}}$ given by

$$\boldsymbol{\Sigma}_{\mathrm{M}} = \begin{bmatrix} \sigma_{R1}^2 & 0 & 0 \\ 0 & \sigma_{R2}^2 & 0 \\ 0 & 0 & \sigma_{\vartheta}^2 \end{bmatrix} \quad (9)$$

where σ_{R1}^2, σ_{R2}^2 and σ_{ϑ}^2 are the variances of the errors on R_{B1}, R_{B2} and ϑ, respectively. In practice, σ_{R1}^2 and σ_{R2}^2 can be derived from the 'a posteriori' error covariance matrix of the Kalman algorithm, separately applied on PCL1 and PCL2; similarly σ_{ϑ}^2 can be estimated as $\sigma_{\vartheta}^2 = (\lambda/2\pi d\cos\vartheta)^2\mathrm{SNR}^{-1}$ where ϑ is the estimated target DoA and the SNR is estimated at the target detection point on the range/Doppler map. Note that it has been reasonably assumed that the cross-covariance between the collected measurements is equal to zero.

Under these hypotheses, the ML estimator for the target position might be derived by solving the following minimisation problem

$$\min_{\boldsymbol{p}} = \Big\{\big[(\boldsymbol{m}-\boldsymbol{m}_0) - \boldsymbol{H}\cdot(\boldsymbol{p}-\boldsymbol{p}_0)\big]^{\mathrm{T}}\boldsymbol{\Sigma}_{\mathrm{M}}^{-1} \big[(\boldsymbol{m}-\boldsymbol{m}_0) - \boldsymbol{H}\cdot(\boldsymbol{p}-\boldsymbol{p}_0)\big]\Big\} \quad (10)$$

that has the following solution

$$\boldsymbol{p} = \left(\boldsymbol{H}^{\mathrm{T}}\boldsymbol{\Sigma}_{\mathrm{M}}^{-1}\boldsymbol{H}\right)^{-1}\boldsymbol{H}^{\mathrm{T}}\boldsymbol{\Sigma}_{\mathrm{M}}^{-1}(\boldsymbol{m}-\boldsymbol{m}_0) + \boldsymbol{p}_0 \quad (11)$$

As is apparent, the target position updating obtained by resorting to the ML estimator depends not only on the collected measurements and the target-sensors geometry, as in (6), but also it depends on the accuracy of the available measurements. Obviously, (11) would coincide with (6) whenever the errors affecting the performed measurements are characterised by the same variance (i.e. $\boldsymbol{\Sigma}_{\mathrm{M}} = \sigma^2\boldsymbol{I}_{3\times 3}$).

Going backwards, the result in (11) would be derived by considering a LS approach applied against the following minimisation problem

$$\min_{\boldsymbol{p}} = \left\{\Sigma_{\mathrm{M}}^{-1/2}\left|\boldsymbol{H}\cdot(\boldsymbol{p}-\boldsymbol{p}_0) - (\boldsymbol{m}-\boldsymbol{m}_0)\right|^2\right\} \quad (12)$$

This is tantamount to the solution of the system in (2) where each equation is weighted according to the accuracy of the corresponding measurement.

The output of the iterative procedure based on the ML estimator for the considered experiment is reported in Fig. 7 (white dots). Better results are obtained with respect to the LS approach since the deviations of the target track from the ground truth are significantly reduced. This is because of a better exploitation of the DoA measurement when solving the system of equations. Basically the use of the different measurements weighted according to their own accuracies suggests to rely mainly on the angular information.

The quantitative analysis of the performance of the ML estimator is reported in Table 1. As is apparent the maximum deviation between the ground truth and the estimated target position reduces to approximately 2.4 m (about 5 m smaller that that given by the LS approach). Similarly the improvements in the mean error and the error standard deviation are 0.5 m and 1.2 m, respectively.

It is worth noting that, using the true ML approach, the inclusion of an additional range measurement yields better

performance with respect to the use of a single range and DoA measurements; this reveals that the system is able to identify the most reliable measurements and exploit all information in the best possible way. Note that this allows us to achieve always the best possible 2D localisation accuracy for the target in any position inside the surveillance area, without requiring to select the best subset of measurements to be used for localisation.

Interestingly enough, the use of the ML intrinsically avoids that the use of noisy information degrades the global 2D localisation accuracy, so that it is generally a viable practical solution. Therefore the ML approach described above can even be nicely extended when the set of exploited measurements is widened by including the Doppler frequencies aiming at estimating also the target's velocity.

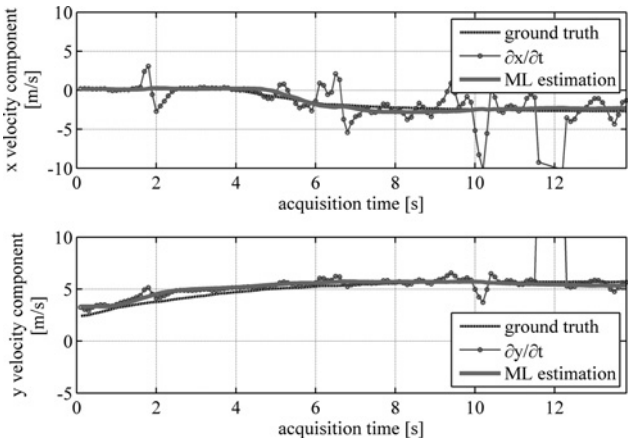

Fig. 8 *Target velocity components estimation*

5 Target's velocity estimation

To obtain an estimate of the target velocity components along the x and y directions, namely v_x and v_y, also the bistatic Doppler frequency measurements should be included in the system of equations in (1) for both the PCL sensors. In fact, the Doppler frequency of the target echo depends on its velocity components $v_x - v_y$ as well as on the system bistatic geometry. Thus the target motion evaluation requires the joint estimation of both the target velocity and the target position. Specifically, the following two equations should be added to the system in (1): (see (13))

Therefore a system of five equations in four unknowns should be solved. Let us define the augmented vector of measurements $\boldsymbol{m}_a = [R_{B1}\ R_{B2}\ \vartheta\ f_{D1}\ f_{D2}]^{\mathrm{T}}$ (5×1), the augmented vector of estimates $\boldsymbol{p}_a = [x_t\ y_t\ v_x\ v_y]^{\mathrm{T}}$ (4×1) and the corresponding matrix $\boldsymbol{H}_a$ (5×4) of partial derivatives evaluated at the tentative point $\boldsymbol{p}_{a0}$. The considered system of equations might be linearised as in (2) and its solution, based on the ML approach, is given by (11) where the matrix structures are replaced with their augmented versions and the covariance matrix $\boldsymbol{\Sigma}_{\boldsymbol{Ma}}$ (5×5) includes the variances of the Doppler frequency measurements.

The results are reported in Fig. 8 along the considered acquisition for both the velocity components compared with the ground truth. For the purpose of our analysis, we have also reported the velocity components obtained as time derivatives of the estimated target x-y coordinates obtained in Section 4.2.

As is apparent, the joint estimation of the target position and velocity based on the ML approach provides much more accurate results with respect to the case of time derivatives of the position components. This is because of the exploitation of the quite accurate Doppler frequency measurements that directly depend on the target motion parameters. In contrast, the estimated target position yields information about its motion only when observed at consecutive time instants; as a consequence, the localisation errors might be doubled when evaluating the target velocity components.

Clearly different approaches might be exploited for the estimation of the target velocity components. Nevertheless the reported results show that the target motion parameters can be reasonably estimated based on the measurements provided by a couple of PCL system dislocated on the surveillance area. This estimate might fruitfully feed the target tracking algorithm over the $x-y$ plane or it can effectively initialise the target motion parameters estimation stage needed for the target cross-range profile formation based on ISAR techniques [23].

6 Conclusions

In this paper the 2D target localisation has been addressed for the case of a WiFi-based PCL system aimed at local area surveillance applications.

Different strategies have been investigated based on different set of measurements possibly provided by multiple PCL receivers. The performance of the considered strategies has been evaluated and compared against real data collected for a vehicular target localisation experiment.

It has been shown that a reasonable target localisation capability is obtained by using the range measurements from two PCL systems; however, to be fruitfully exploited,

$$\begin{cases} f_{D1} = \dfrac{1}{\lambda}\left[\dfrac{(x_{\mathrm{TX}}-x_t)v_x}{\sqrt{(x_{\mathrm{TX}}-x_t)^2+(y_{\mathrm{TX}}-x_t)^2}} + \dfrac{(y_{\mathrm{TX}}-y_t)v_y}{\sqrt{(x_{\mathrm{TX}}-x_t)^2+(y_{\mathrm{TX}}-x_t)^2}} + \dfrac{(x_1-x_t)v_x}{\sqrt{(x_1-x_t)^2+(y_1-x_t)^2}} + \dfrac{(y_1-y_t)v_y}{\sqrt{(x_1-x_t)^2+(y_1-x_t)^2}}\right] \\ f_{D2} = \dfrac{1}{\lambda}\left[\dfrac{(x_{\mathrm{TX}}-x_t)v_x}{\sqrt{(x_{\mathrm{TX}}-x_t)^2+(y_{\mathrm{TX}}-x_t)^2}} + \dfrac{(y_{\mathrm{TX}}-y_t)v_y}{\sqrt{(x_{\mathrm{TX}}-x_t)^2+(y_{\mathrm{TX}}-x_t)^2}} + \dfrac{(x_2-x_t)v_x}{\sqrt{(x_2-x_t)^2+(y_2-x_t)^2}} + \dfrac{(y_2-y_t)v_y}{\sqrt{(x_2-x_t)^2+(y_2-x_t)^2}}\right] \end{cases} \tag{13}$$

doi: 10.1049/iet-rsn.2013.0207

such measurements should be taken after the application of a tracking stage in the bistatic range/Doppler plane.

Besides, the joint exploitation of bistatic range and DoA measurements has been shown to yield improved 2D localisation performance thanks to the higher accuracy provided by the angular information. This gives a hint for the design of a multistatic WiFi-based PCL system that should preferably include few sensors equipped with multiple receiving antennas, instead of many lower-cost sensors based on a single surveillance antenna.

It has also been shown the importance of knowing the accuracy of the available measurements, that need to be taken into account when exploiting a higher number of measurements. As apparent this enables the use of a true ML approach for the target position estimation. This allows to gather the highest benefits from all the available measurements, thus exploiting full multistatic passive radar configurations to provide the highest possible 2D localisation accuracy.

Finally, the ML approach has been extended to the target motion components estimation stage aiming at increasing the monitoring capabilities of the conceived system. This is also very useful for the subsequent potential processing stages of either target tracking, or cross-range target profiling by means of ISAR techniques.

Although further improvements are expected if a wider network of properly displaced receivers is used to collect a wider set of range/Doppler/DoA measurements, the reported results clearly demonstrate that there are good potentialities for the WiFi-based PBR for short range surveillance to provide accurate 2D location of vehicular targets, despite the wide antenna beams typically used by such sensors.

7 Acknowledgment

This work has been carried out under the support of the Project FP7-PEOPLE-2011-IAPP: SOS – 'Sensors system for detection and tracking of dangerous materials in order to increase the airport Security in the indoor landside area' funded by the European Union.

8 References

1 Special no. on Passive Radar Systems, IEE Proceedings on Radar, Sonar and Navigation, June 2005, vol. 152, no. 3, pp. 106–223
2 Lombardo, P., Colone, F.: 'Advanced processing methods for passive bistatic radar systems', in Melvin, W.L., Scheer, J.A. (Eds.): 'Principles of Modern Radar: Advanced Techniques' (SciTech Publishing, 2012, 1st edn.)
3 Tan, D.K.P., Sun, H., Lu, Y., Lesturgie, M., Chan, H.L.: 'Passive radar using global system for mobile communication signal: theory, implementation and measurements'. IEE Proc. – Radar, Sonar and Navigation, June 2005, vol. 152, no. 3, pp. 116–123
4 Krysik, P., Kulpa, K., Baczyk, M., Maslikowski, L., Samczynski, P.: 'Ground moving vehicles velocity monitoring using a GSM based passive bistatic radar'. Proc. 2011 IEEE CIE Int. Conf. on Radar, Chengdu, China, October 2011, vol. 1, pp. 781–784
5 Krysik, P., Samczynski, P., Malanowski, M., Maslikowski, L., Kulpa, K. S.: 'Velocity measurement and traffic monitoring using a GSM passive radar demonstrator', *IEEE Aeros. Electron. Syst. Mag.*, 2012, **27**, (10), pp. 43–51
6 Zemmari, R., Nickel, U., Wirth, W.D.: 'GSM passive radar for medium range surveillance'. Proc. 2009 European Radar Conf. – EuRAD 2009, Rome, Italy, September–October 2009, pp. 49–50
7 Nickel, U.: 'System considerations for passive radar with GSM illuminators'. Proc. 2010 IEEE Int. Symp. on Phased Array Systems and Technology, Waltham, MA, USA, October 2010, pp. 189–195
8 Zemmari, R., Daun, M., Nickel, U.: 'Maritime surveillance using GSM passive radar'. Proc. 13th Int. Radar Symp. – IRS 2012, Warsaw, Poland, May 2012, pp. 76–82
9 Weiss, M.: 'Passive WLAN radar network using compressed sensing'. Proc. IET Int. Conf. on Radar Systems (Radar 2012), Glasgow, UK, October 2012, pp. 1–6
10 Colone, F., Falcone, P., Lombardo, P.: 'Ambiguity Function Analysis of WiMAX Transmissions for Passive Radar'. Proc. 2010 IEEE Radar Conf., Washington, D.C., USA, May 2010, pp. 689–694
11 Chetty, K., Woodbridge, K., Guo, H., Smith, G.E.: 'Passive bistatic WiMAX radar for marine surveillance'. Proc. 2010 IEEE Radar Conference, Washington, D.C., USA, May 2010, pp. 188–193
12 Colone, F., Woodbridge, K., Guo, H., Mason, D., Baker, C.J.: 'Ambiguity function analysis of wireless LAN transmissions for passive radar', *IEEE Trans. Aerosp. Electron. Syst.*, 2011, **47**, (1), pp. 240–264
13 Colone, F., Falcone, P., Bongioanni, C., Lombardo, P.: 'WiFi-based passive bistatic radar: data processing schemes and experimental results', *IEEE Trans. Aerosp. Electron. Syst.*, 2012, **48**, (2), pp. 1061–1079
14 Chetty, K., Smith, G.E., Woodbridge, K.: 'Through-the-wall sensing of personnel using passive bistatic WiFi radar at standoff distances', *IEEE Trans. Geosci. Remote Sens.*, 2012, **50**, (4), pp. 1218–1226
15 Falcone, P., Colone, F., Lombardo, P.: 'Potentialities and challenges of WiFi-based passive radar', *IEEE Aerosp. Electron. Syst. Mag.*, 2012, **27**, (11), pp. 15–26
16 Colone, F., Falcone, P., Lombardo, P.: 'Passive bistatic radar based on mixed DSSS and OFDM WiFi transmissions'. Proc. 2011 European Radar Conf. – EuRAD 2011, Manchester, UK, October 2011, pp. 154–157
17 Falcone, P., Colone, F., Bongioanni, C., Lombardo, P.: 'Experimental results for OFDM WiFi-based passive bistatic radar'. Proc. 2010 IEEE Radar Conf., Washington, D.C., USA, May 2010, pp. 516–521
18 Falcone, P., Colone, F., Lombardo, P., Bucciarelli, T.: 'Range sidelobes reduction filters for WiFi-based passive bistatic radar'. Proc. 2009 European Radar Conf. – EuRAD 2009, Rome, Italy, September–October 2009, pp. 133–136
19 Falcone, P., Colone, F., Lombardo, P.: 'Doppler frequency sidelobes level control for WiFi-based passive bistatic radar'. Proc. 2011 IEEE Radar Conf., Kansas City, MO, USA, May 2011, pp. 435–440
20 Chetty, K., Smith, G., Guo, H., Woodbridge, K.: 'Target detection in high clutter using passive bistatic WiFi radar'. Proc. 2009 IEEE Radar Conf., Pasadena, CA, USA, May 2009, pp. 1–5
21 Falcone, P., Colone, F., Macera, A., Lombardo, P.: 'Localization and tracking of moving targets with WiFi-based passive radar'. Proc. 2012 IEEE Radar Conference, Atlanta, GA, USA, May 2012, pp. 705–709
22 Falcone, P., Colone, F., Lombardo, P.: 'Localization of moving targets with passive radar system based on WiFi transmissions'. Proc. IET Int. Conf. on Radar Systems (Radar 2012), Glasgow, UK, October 2012, pp. 1–6
23 Colone, F., Pastina, D., Falcone, P., Lombardo, P.: 'WiFi-based passive ISAR for high resolution cross-range profiling of moving targets', *IEEE Trans. Geosci. Remote Sens.*, In press, doi: 10.1109/TGRS.2013.2273099
24 Falcone, P., Colone, F., Lombardo, P., Pastina, D.: 'WiFi-based passive ISAR for high resolution cross-range profiling of moving targets'. Proc. Ninth European Conf. on Synthetic Aperture Radar 2012 – EUSAR 2012, Nuremberg, Germany, April 2012, pp. 279–282
25 Falcone, P., Pastina, D., Colone, F., Macera, A., Lombardo, P.: 'Advances in ISAR processing for High Resolution Cross-Range Profiling with Passive Radar'. Proc. 13th Int. Radar Symp. – IRS 2012, Warsaw, Poland, May 2012, pp. 421–425
26 Colone, F., Falcone, P., Macera, A., Lombardo, P.: 'High resolution cross-range profiling with Passive Radar via ISAR processing'. Proc. 12th Int. Radar Symp. – IRS 2011, Leipzig, Germany, September 2011, pp. 301–306
27 Colone, F., O'Hagan, D.W., Lombardo, P., Baker, C.J.: 'A multistage processing algorithm for disturbance removal and target detection in passive bistatic radar', *IEEE Trans. Aerosp. Electron. Syst.*, 2009, **45**, (2), pp. 698–722
28 Daun, M., Nickel, U., Koch, W.: 'Tracking in multistatic passive radar systems using DAB/DVB-T illumination', *Signal Process.*, 2012, **92**, (6), pp. 1365–1386
29 Battistelli, G., Chisci, L., Morrocchi, S., Papi, F., Farina, A., Graziano, A.: 'Robust multisensor multitarget tracker with application to passive multistatic radar tracking', *IEEE Trans. Aerosp. Electron. Syst.*, 2012, **48**, (4), pp. 3450–3472
30 Kaplan, E., Hegarty, C. (Eds.): 'Understanding GPS Principles and Applications' (Artech House, 1996, 2nd edn.)